Molecular Vision 2019; 25:183-193 <http://www.molvis.org/molvis/v25/183>
Received 27 August 2018 | Accepted 15 March 2019 | Published 17 March 2019

Differential stability of variant *OPN1LW* gene transcripts in myopic patients

Jessica K. Mountford,[1,2,3,4] Wayne I. L. Davies,[1,2,3,4] Lyn R. Griffiths,[5] Seyhan Yazar,[1,6] David A. Mackey,[1] David M. Hunt[1,2]

[1]Centre for Ophthalmology and Visual Science, Lions Eye Institute, University of Western Australia, Perth, WA, Australia; [2]School of Biological Sciences, University of Western Australia, Perth, WA, Australia; [3]UWA Oceans Institute, University of Western Australia, Crawley, WA, Australia; [4]Oceans Graduate School, University of Western Australia, Crawley, WA, Australia; [5]Genomics Research Centre, Institute of Health and Biomedical Innovation, Queensland University of Technology, Brisbane, QLD, Australia; [6]MRC Human Genetics Unit, Institute of Genetics and Molecular Medicine, University of Edinburgh, Edinburgh, UK

Purpose: In Bornholm eye disease, a defect in the splicing of transcripts from a variant *OPN1LW* opsin gene leads to a depletion in spliced transcript levels and, consequently, a reduction in photopigment in photoreceptors expressing the variant gene.

Methods: Myopic and age-matched control subjects were drawn from the Western Australian Pregnancy Cohort (Raine) Study and the Norfolk Island Eye Study groups. The *OPN1LW* opsin gene was amplified using long-range PCR methodology and was fully sequenced. Expression of variant opsins was evaluated using quantitative PCR (qPCR). RNA secondary structure changes arising from identified variants were predicted by modeling.

Results: Forty-two nucleotide sites were found to vary across the 111 subjects studied. Of these, 15 had not been previously reported, with three present only in myopic individuals. Expression of these variants in transfected human embryonic kidney (HEK293T) cells demonstrated that splicing efficiencies were not affected. However, gene transcripts from two of the three variants were significantly depleted. RNA secondary structure modeling predicted that these single nucleotide changes could affect RNA stability.

Conclusions: None of the variants identified in myopic individuals appeared to alter the efficiency of transcript splicing. However, two resulted in a significant reduction in the number of spliced and unspliced transcripts, indicating an overall reduction in steady-state transcript stability. Such a change would be expected to result in a reduced amount of photopigment, and this may be a contributing factor in the development of myopia.

Myopia, or near-sightedness, is a common refractive defect of the eye. It arises from excessive axial elongation such that the image is focused in front of the retina when accommodation is relaxed. High-grade myopia with a refractive error of −5.00 diopters (D) or worse is more frequently associated with pathological myopia and blindness due to premature cataracts, glaucoma, retinal detachment, and chorioretinal degeneration. The prevalence of myopia varies in different countries, with rates of 17% in Australia, 26% in USA, and 27% in Western Europe [1, 2], but much higher frequencies are found in Asian countries, with rates of 71%–96% reported [3, 4]. The prevalence has increased significantly in recent years, indicating that we are facing a global epidemic of myopia [5].

The genetic basis for myopia has been the subject of several studies. Several genetic loci for high-grade and moderate myopia have been identified, mostly from studies of family pedigrees [6]. In addition, genome-wide association studies have identified a large number of genetic loci associated with myopia [7-9]. Among these is the *MYP1* (Gene ID 4657; OMIM 310460) locus, which maps to the tip of the X chromosome at Xq28 [10]. *MYP1* is associated with the X-linked cone dysfunction disorder Bornholm eye disease (BED), named after the five-generation family from the Danish island of Bornholm in which the disorder was first identified [11]. BED is described as a stationary cone dysfunction syndrome characterized by myopia, acuity loss, and dichromacy, with either protanopia or deuteranopia described in different families [12]. This disorder differs, therefore, from the common form of dichromacy, in which only red–green color vision is affected and visual acuity is fully preserved.

BED was the subject of a detailed study [13] that showed that several families possessed an *OPN1LW* (Gene ID 5956; OMIM 300822) gene (also referred to as the "human L cone opsin gene"), which encodes a photopigment containing a rare five–amino acid haplotype in exon 3. In vitro expression in transfected cultured cells showed that the variant opsins

Correspondence to: David M Hunt, Lions Eye Institute, University of Western Australia, Crawley, WA 6009, Australia; Phone: 61 416236109; FAX: 61 8 9381 0700; email: david.hunt@uwa.edu.au

formed functional photopigments— albeit with shifts of up to 10 nm in their spectral maxima—that trafficked to the cell membranes. As such, it is unlikely that dysfunctional photopigments underlie the pathology. The alternative is that the nucleotide changes in the gene that are responsible for the novel amino acid haplotype in exon 3 affect the splicing of the *OPN1LW* gene transcript [14]. A splicing defect has now been confirmed as the process that affects photopigment production in BED [15-17].

In BED patients, cones that express the *OPN1LW* gene with the rare haplotype in exon 3 are affected by *OPN1LW* splicing defects, leading to a severe reduction in or complete loss of photopigment production; this ultimately results in the dysfunction and loss of cones. In confirmation of this, an individual with one of the rare *OPN1LW* haplotypes has been shown by adaptive optics [18] to have areas within the cone mosaic that lack cones, suggesting that cones are lost some time after foveal migration. In "normal" dichromats with a fully functional gene, such gaps are not observed, and the cone mosaic is indistinguishable from that observed in normal trichromats [19]. It would appear, therefore, that the presence of aberrant cones can impact on emmetropization, the process that guides ocular growth toward the optimal optical state. Eye length is regulated by visual experience and develops to match the optics of the eye, as well as to compensate for variation in corneal/lens curvature and power [20]. The signals that guide this process are initiated largely by light absorption of the photopigments found in both L and M cones, with the latter expressing the *OPN1MW* (Gene ID 2652; OMIM 300821; or M cone opsin) gene. Changes in the pattern of light and dark in the retinal image that characterize blurred versus sharply focused images are monitored to stop eye growth when the correct length for coordinated plano (neutral) optics is reached. In BED patients, the emmetropization process malfunctions as a result of opsin photopigment variation and a change in the organization of the cone mosaic [18]. Myopia arises, therefore, from the presence of variant opsin genes and their altered gene products; this was confirmed by a recent study of several *MYP1* families [21] in which unique variants in the *OPN1LW* gene were shown to be present.

The *OPN1LW* and *OPN1MW* genes are among the most variable genes in the human genome, with many variants arising from their head-to-tail organization within an X chromosome array [22]. This leads to mispairing at meiosis and unequal crossing over within the gene array [23]. It is possible, therefore, that other variants will also alter, to varying extents, the functionality of cones expressing these photopigments, and that this will have an impact on the process of emmetropization of the eye, leading to different severities of myopia. In this study, the *OPN1LW* gene was sequenced in two cohorts of individuals, the Western Australian Pregnancy Cohort (Raine) Study group and the Norfolk Island Eye Study group; in both groups, myopic individuals were identified and fully assessed.

METHODS

Ethics: For all subjects, the research presented here adhered to the tenets of the Declaration of Helsinki. The protocol was approved by the Human Ethics Committees of the University of Western Australia and Royal Victorian Eye and Ear Hospital in Melbourne, Australia. Informed written and verbal consent was obtained from all subjects.

Study cohorts: The Western Australian Pregnancy Cohort (Raine) Study was established in 1989 with participants drawn from births registered from 1989 to 1992 at the King Edward Memorial Hospital in Perth, Western Australia [24]. The children were assessed at birth and at one year, two years, three years, and five years of age. Information on their height, weight, eating habits, walking, talking, behavior, and any medical conditions or illnesses was collected. The group now comprises 2358 participants who are aged 25–28 years. Between 2010 and 2012, a total of 1344 participants had a comprehensive ophthalmological examination, including assessment for refractive errors [25], with 23.7% being myopic (less than −0.5 D) at the 20-year follow-up.

The Norfolk Island Eye Study took place on Norfolk Island, a remote Australian territory in the South Pacific Ocean. More than 40% of its inhabitants can trace their origins over 12 generations to the originating founders—12 Tahitian women and six European men—who came to reside on Pitcairn Island following the infamous mutiny on HMS Bounty [26]. The majority of the Pitcairn Island residents subsequently moved to Norfolk Island. It is estimated that the permanent Norfolk Island population has a gene pool that is 88% of European ancestry and 12% of Polynesian ancestry (Territories Norfolk). The eye study project was initiated in 2007. Assessment of refractive errors in 677 individuals (367 females and 310 males) of this population revealed that the prevalence of myopia (<−1.0 D) is 10% [27].

Sequencing of OPN1LW gene: The *OPN1LW* gene was PCR amplified from genomic DNA (gDNA) using the primers listed in Appendix 1. The first step was a long-range PCR (LRP) using Bioline RANGER (Bioline, Alexandria, NSW, Australia) with forward primers FG targeted to the upstream promoter region of the first gene in the L/M cone opsin array and reverse primer E6 targeted specifically to exon 6, which is highly conserved in both the *OPN1LW* and *OPN1MW* genes.

Cycling conditions were 93 °C for 3 min, then 10 cycles of 93 °C for 15 s, 62 °C for 30 s, and 68 °C for 15 min, followed by 18 cycles of 93 °C for 15 s, 62 °C for 30 s, and 68 °C for 15 min (20 s increments for each cycle). A second PCR was then set up using 1 µl (50–100 ng) of amplified DNA from the first PCR as a template and MyTaq DNA polymerase (Bioline, Alexandria, NSW, Australia). As exons 1 and 6 are identical for *OPN1LW* and *OPN1MW*, gene-specific primers were limited to exons 2, 3, 4, and 5. PCR conditions were as follows: an initial 95 °C for 3 min, then 35 cycles of 94 °C for 45 s, 60 °C for 45 s, and 72 °C for 1 min, followed by 72 °C for 7 min. Discrete exon 2 to exon 5 amplicons were separated by agarose gel electrophoresis, and excised and purified using a QIAquick Gel Extraction Kit (Qiagen, Chadstone, VIC, Australia) before sequencing in both directions by the Australian Genome Research Facility (AGRF, Perth, Western Australia, Australia). Sequences were aligned and compared to the reference *OPN1LW* gene sequence (NM_020061.5), and variants were detected using Codon Code Aligner version 6.0.1 software (CodonCode Corporation, Centerville, MA).

Site-directed mutagenesis and cloning: Exons 1 to 6, including introns 4 and 5 of the wild-type (WT) *OPN1LW* gene, were amplified separately from 50 to 100 ng of gDNA using primers designed specifically to the exon/intron boundary of interest (Appendix 1). Once amplified, these amplicons were used to generate several full-length constructs containing the "spliced" coding sequences, but retaining the introns of choice, with or without the desired variants detailed below. To achieve this, the SPLICE technique was applied, as described previously [28]. Briefly, the first-round amplification was performed using KOD Hot Start DNA polymerase (Merck Millipore, Bayswater, VIC, Australia) and 1 µl (50–100 ng) gDNA as template. Cycling conditions consisted of an initial 95 °C for 2.5 min, followed by 40 cycles of 95 °C for 30 s, 55 °C for 30 s, and 68 °C for 1.5 min. The second-round amplification stage used equimolar concentrations of purified PCR products from the first round of amplification as a template; this stage consisted of an initial 95 °C for 2 min, followed by 40 cycles of 95 °C for 30 s, 55 °C for 30 s, and 68 °C for 2.5 min. The third and fourth rounds of amplification consisted, respectively, of an equimolar concentration of purified second and third round PCR products as template, with of an initial 95 °C for 2 min, followed by 40 cycles of 95 °C for 30 s, 55 °C for 30 s, and 68 °C for 3.5 min.

Sequencing the *OPN1LW* gene from myopic patients revealed several novel variants that were not present in control subjects. To introduce these single-nucleotide variants into the WT *OPN1LW* gene construct described above, site-directed mutagenesis was applied using the SPLICE technique stated above and described previously [28]. Specifically, forward and reverse primers were designed (Appendix 1), covering the region containing the variant. The first-round PCR amplification stage used KOD Hot Start DNA polymerase to amplify 1 µl (50–100 ng) of the WT *OPN1LW* gene construct as a template, using a forward primer over the translation start codon (PE-L-cone-F) paired with a reverse-variant primer. In a separate reaction, a forward-variant primer was used with a reverse primer over the translation stop codon (PE-L-cone-R). Cycling conditions consisted of an initial 95 °C for 2 min, followed by 40 cycles of 95 °C for 30 s, 60 °C for 15 s, and 68 °C for 3.5 min. The second-round amplification stage used equimolar concentrations of purified first round variant PCR products as template, using flanking forward and reverse primers (PE-L-cone-F and PE-L-cone-R), and consisted of an initial 95 °C for 2 min, followed by 40 cycles of 95 °C for 30 s, 60 °C for 15 s, and 68 °C for 3.5 min. The two amplification stages resulted in single, discrete amplicons containing full-length *OPN1LW* gene variant sequences, with both EcoRI and SalI restriction sites at the 5′- and 3′-ends of the coding region. Following restriction enzyme digestion, purified fragments were ligated into the mammalian expression vector pMT4 [29], using T4 DNA ligase (Genesearch, Arundel, QLD, Australia). They were subsequently transfected into chemically competent cells (α-Select Silver Efficiency; Bioline, Alexandria, NSW, Australia), as previously described [30-33]. Correct clones were determined using Sanger sequencing (AGRF, Perth, WA, Australia) to ensure sequence fidelity.

Transfection of OPN1LW mini-genes: Human embryonic kidney (HEK293T) cells were transiently transfected in triplicate with 1.2 µg of *OPN1LW*-pMT4 recombinant expression vector using Attractene (Qiagen, Chadstone, VIC, Australia) in six-well cell culture plates. After 48 h, transfected cells were harvested using Trypsin-EDTA 1X (Sigma-Aldrich, Castle Hill, NSW, Australia), and washed four times with PBS (1X; 138 mM NaCl, 2.70 mM KCl, 10 mM $NaPO_4$, 1.8 mM KPO_4, pH 7.4). Total RNA was extracted using the PureLink RNA Mini with the TRIzol kit (Thermo Fisher Scientific, Scoresby, VIC, Australia), before the generation of oligo dT-primed cDNA using 5 µl (1–2 µg) of total RNA incubated with 5 µl oligo dT (500 ng) and 20.5 µl sterile RNase-free water for 15 min at 85 °C, followed by 2 min on ice. Subsequently, 10 µl of 5X First-Strand Buffer (Genesearch, Arundel, QLD, Australia), 5 µl (0.1 M) of DTT (Genesearch, Arundel, QLD, Australia), 2.5 µl (10 mM) dNTP mix (Bioline, Alexandria, NSW, Australia), and 1 µl RNase murine inhibitor (40 U/µl; Genesearch, Arundel, QLD, Australia) was added and incubated for 2 min at 25 °C.

Then, 1 µl of M-MuLV Reverse Transcriptase (Genesearch, Arundel, QLD, Australia) was added and incubated for a further 5 min at 25 °C, followed by 1 h at 42 °C. Finally, a further 1 µl of M-MuLV Reverse Transcriptase (Genesearch, Arundel, QLD, Australia) was added and incubated for another 1 h at 42 °C.

Quantitative PCR of OPN1LW mini-gene transcripts: Once generated, RNA from transfected cells was extracted and quantified. Resultant cDNA (100 ng) was used to determine the levels of expression of *OPN1LW* gene transcripts derived from WT and variant constructs. This was achieved using a commercial quantitative PCR (qPCR) kit (SYBR Green PCR Master Mix; Qiagen, Chadstone, VIC, Australia) and 10 µM of the final concentration of each forward and reverse primer (Appendix 1; all qPCR primers were designed using ApE - A Plasmid Editor version 1.10.4 [M.W. Davis, University of Utah, Salt Lake City, UT]). All transient transfection experiments were conducted at least in triplicate to ensure a minimum of three biologic replicates were used.

In addition, all qPCR experiments were performed at least three times on a 72 Well Rotor-Gene Q Real-Time PCR instrument (Qiagen, Chadstone, VIC, Australia), using the following three-step cycling pipeline: 95 °C for 5 min, followed by 40 cycles of 95 °C for 5 s, 61 °C for 10 s, and 77 °C (primer sets 6 [Elongation factor 1 alpha – *EFIA*] (Gene ID 3189; OMIM 130590), 7 [13 [3′-untranslated region (UTR) of 215 the OPN1LW mRNA]) ribosomal protein L13A- *RPL13A*] (Gene ID: 23521, OMIM 610173), and 13 [3′-untranslated region (UTR) of the *OPN1LW* mRNA]) or 80 °C (primer sets 2 [Ex4-In4], 3 [In4-Ex5], 4 [Ex5-In5], 5 [In5-Ex6], 6 [EFIA], 9 [In1-In1], 10 [In2-In2], 11 [In3-In3], and 12 [5′-UTR of the *OPN1LW* mRNA]) for 5 s. Note that the final cycling temperatures of 77 °C and 80 °C were used to remove all potential traces of contaminating primer dimer. Also, qPCR experiments were performed to amplify regions within the 5′- and 3′-UTRs, and introns 1, 2, and 3, to monitor the expression of any endogenous *OPN1LW* gene activity; this was done because these parts of the transcript were absent in all transfected constructs. Two housekeeping genes, *RPL13A* and *EFIA1,* were also included to serve as internal controls.

Following previous protocols [31, 34], primers were designed to produce amplicons of <250 bp in length. According to standard qPCR practice, the target specificity and annealing/PCR efficiency of each primer set was determined at the cycling conditions described above that were optimal, with primer efficiencies close to 100%. Primer efficiencies were determined by standard curve analysis (a semi-log plot of the PCR cycle value above the designated background threshold value, against the log of input cDNA concentration), with five known concentrations (0.01 ng, 0.1 ng, 1 ng, 10 ng, and 100 ng), to demonstrate that all primer pairs were efficient over a magnitude of 1×10^5, as previously described [31, 34]. Once data were collected, the baseline and threshold values automatically determined by the Rotor-Gene software version 2.3 (Qiagen, Chadstone, VIC, Australia) were manually checked, before cycle threshold (Ct) values were exported to a Microsoft Excel spreadsheet. The geometric mean of the two housekeeping genes was calculated and used to normalize target gene expression and correct for sample-to-sample variation [31, 35]. All data were analyzed offline, using a method adapted from Carleton and Kocher [36], where the relative expression (RE) of the WT *OPN1LW* gene and variant transcripts (RE_{Lcone}) compared to that of internal controls (RE_{int}; described above) was calculated as follows:

Relative expression of target $(RE_{Lcone}/RE_{int}) = c \times[(1 + E_{int})^{(Ct_{int})}]/[(1 + E_{Lcone})^{(Ct_{Lcone})}]$, where E_{Lcone} and E_{int} are the primer efficiencies of each individual *OPN1LW* gene target and the internal control (geometric mean of *RPL13A* and *EF1A1* expression levels), respectively, and Ct_{Lcone} and Ct_{int} are the experimentally determined Ct values for each individual *OPN1LW* gene target and the internal control (geometric mean of *RPL13A* and *EF1A1*), respectively. In all cases, an arbitrary multiplication constant (c) of 10^9 was used.

Bioinformatic analysis: RNA secondary structures containing exonic regions of WT and variant *OPN1LW* gene transcripts were predicted using mfold version 3.6 (UNAfold) [37, 38]. The complex algorithm developed by Zuker and colleagues [37, 38] initially predicts the secondary structure of a linear RNA sequence to generate an initial Gibbs free energy value (ΔG, with SI units kcal mol^{-1}), which represents the change in Gibbs free energy for a given system at 37 °C. In this context, the ΔG value is a proxy for how much total energy is required to break each loop to form a linear single strand of RNA (or similarly, the amount of energy released during secondary structure formation). Once predicted, the mfold algorithm re-evaluates the initial predictions using more sophisticated rules (e.g., application of the Jacobson-Stockmeyer theory to assign free energies to multi-branch loops that includes a term that grows logarithmically with the number of unpaired bases in the loop and by computing coaxial stacking of adjacent helices in multi-branch loops) to generate one or more RNA secondary structures that contain optimal folding with modified ΔG values that are more accurate than are the initial determined values [37, 38]. As a comparison between the WT and variant predictions, RNA secondary structures with the largest (i.e., most optimal) ΔG values are presented.

Table 1. Nucleotide variants unique to myopia patients.

Variant	Nucleotide site	Nucleotide substitution	Codon	Amino acid substitution	Number of individuals
1	973	A>G	325	Met>Val	1
2	970	T>A	324	Phe>Ile	1
3	971	T>A	324	Phe>Tyr	4

RESULTS

Only males with high-grade myopia (refractive error of <-6.0 D) were included, which comprised 20 myopic and 36 emmetropic controls drawn from the Raine Study's 20-year follow-up, and 25 myopic and 30 emmetropic controls drawn from the Norfolk Island Eye Study group. Genomic DNA was used to PCR amplify across the entire *OPN1LW* gene using gene-specific primers (Appendix 1), as outlined previously. The resulting long amplicons were then used as templates to PCR amplify exons 2, 3, 4, and 5 separately, using exon-specific primers. Exons 1 and 6 were not studied, as they are conserved between the *OPN1LW* and *OPN1LW* genes.

OPN1LW gene variants: Nucleotide variants in the *OPN1LW* gene were identified by comparison to the reference *OPN1LW* gene sequence (NM_020061.5). A total of 42 nucleotide sites were found to vary; of these, 27 have been previously reported (as reported on *Ensembl*) and 15 are novel (ENSG00000102076; r=X:154144224-154159032; v=rs782484270; vdb=variation; vf=147984596). The full list of variants shown in Appendix 2 includes coding and non-coding changes, as both can affect mRNA stability and splicing. Note the high frequency of variants per individual, confirming the high frequency of variants in the *OPN1LW* gene as observed in the general population. Of 111 individuals analyzed, only 1 possessed the full reference sequence. Three nucleotide variants that differed from the reference sequence, c.453A>G (p.Arg151ARg), c.457A>C (p.Met1531Leu), 283 and c.465>G (p.Val155Val) were common throughout both cohorts. Only 24 individuals had the reference haplotype of A453/A457/C465, compared to 80 with the G453/C457/G465, and a further 7 had other combinations at these sites. Eighteen individuals, all from the Norfolk Island cohort, possessed both haplotypes, indicating that at least two *OPN1LW* genes that differ at these three sites were present within the X-chromosome gene array in these individuals.

Note that individuals from the Norfolk Island Eye Study had a much higher frequency of "heterozygosity" at variant sites. Because only male subjects were studied, this indicates a much higher frequency of multiple copies of the *OPN1LW* gene in the X chromosome gene array. The presence of multiple copies of X-linked opsin genes is not uncommon, as reported previously [23]. However, in this case, this higher incidence of multiple copies of the *OPN1LW* gene among the residents of the Norfolk Island cohort may reflect a founder effect arising from the small number of individuals that originally came to reside on Pitcairn Island and were subsequently moved to Norfolk Island (see Territories Norfolk).

Among the 42 variant sites, three novel variants were identified, c.973A>G (p.Met325Val) (variant 1 [V1]), c.970T>A (p.Phe324Ile) (variant 2 [V2]), and c.971T>A (p.Phe324Tyr) (variant 3 [V3]), all from the Raine Study, that were only present in individuals with myopia (Table 1). All were in exon 5, at adjacent codons 324 and 325.

Expression of novel OPN1LW variants in vitro: To assess whether any of the three variants (V1–V3) in exon 5 affect RNA splicing or transcript stability, each was introduced separately by site-directed mutagenesis and the SPLICE technique [28] into a modified WT *OPN1LW* mini-gene that lacked introns 1–3. This was inserted into the mammalian expression vector pMT4 and transfected into HEK293T cells. PolyA$^+$ RNA transcripts from transfected cells were then isolated and converted into cDNA for use as a template in a series of qPCR experiments to assess both splicing and stability. Transient transfection was preferred over the generation of stably transfected cell lines in which expression variation due to different sites of genome insertion may occur, as well as the well-known reduction in overall expression with stable cell lines.

PCR primers targeted to introns 4 and 5 were used to assess the levels of unspliced transcripts. As shown in Figure 1A, the Relative Expression (RE) levels, as measured by all primer combinations in comparison to WT, were significantly lower in V1 and V2, but not in V3. Estimates of spliced transcript levels were obtained from qPCRs that targeted exons 4 to 5 and exons 5 to 6, where PCR conditions were chosen so that amplicons containing large introns (i.e., introns 4 and 5) would not be amplified. As shown in Figure 1B, the levels were again significantly depressed in V1 and V2, but not in V3.

Table 2 shows the levels of spliced and unspliced transcripts plus the proportion of spliced to unspliced

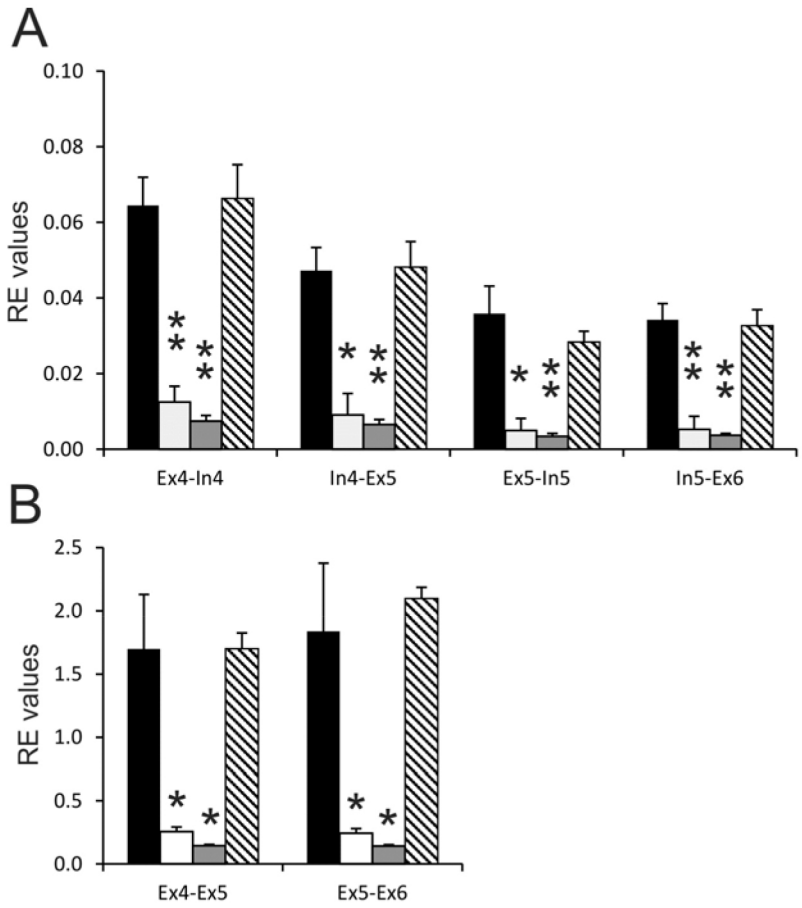

Figure 1. *OPN1LW* gene transcripts expressed in transiently transfected human embryonic kidney (HEK293T) cells. **A**: Relative expression (RE) levels of unspliced transcripts determined by qPCR across the following boundaries: exon 4 – intron 4; intron 4 – exon 5; exon 5 – intron 5; and intron 5 – exon 6. **B**: Relative levels of spliced *OPN1LW* gene transcripts, measured by qPCR, using primer sets that generate amplicons form exon 4 – exon 5 and exon 5 – exon 6. In all cases, the RE values represent *OPN1LW* mRNA expression normalized to the geometric mean of two internal control genes, *RPL13A* and *EF1A1*. Wild-type (WT), black; variant 1 (V1), white; variant 2 (V2), gray; variant 3 (V3), hatched. * and ** denote statistical significance at 1% and 5% probability levels, respectively.

transcripts. For V1 and V2, the total transcript levels (i.e., spliced and unspliced transcripts) were substantially reduced compared to WT, whereas for V3, the level is marginally above WT. In contrast, compared to WT, the proportion (%) of unspliced transcript is marginally higher for V1 and V2, and marginally lower for V3. It would appear, therefore, that for V1 and V2, the combined levels of unspliced and spliced transcripts were significantly depressed compared to WT, whereas the ratio of unspliced to spliced was essentially the same for WT and all three variants (Table 2). This indicates that the sequence differences between V1, V2, and V3 do not affect the splicing process but that V1 and V2 both reduce the overall level of transcripts present at a steady state. Because the transcription of each variant sequence is driven by the same promoter, the reduced relative levels of V1 and V2 transcripts most likely reflect a change in RNA stability.

Table 2. Relative expression (RE) of spliced and unspliced transcripts.

Transcript	WT	Variants		
		V1	V2	V3
Spliced RE	3.534±0.969	0.502±0.073 *	0.288±0.022 **	3.798±0.188
Unspliced RE	0.112±0.013	0.022±0.010 **	0.014±0.003 **	0.115±0.015
% Unspliced	3.16%	4.30%	4.84%	3.02%

The spliced values are the sum of the individual values obtained from qPCR across exons 4–5 and 5–6. The unspliced values are the average of the Ex4 -In4 and In4-Ex5 qPCR values plus the average of the Ex5-In5 and In5-Ex6 qPCR values. Statistically significant differences to WT at 5% (*) and 1% (**) probability levels are indicated.

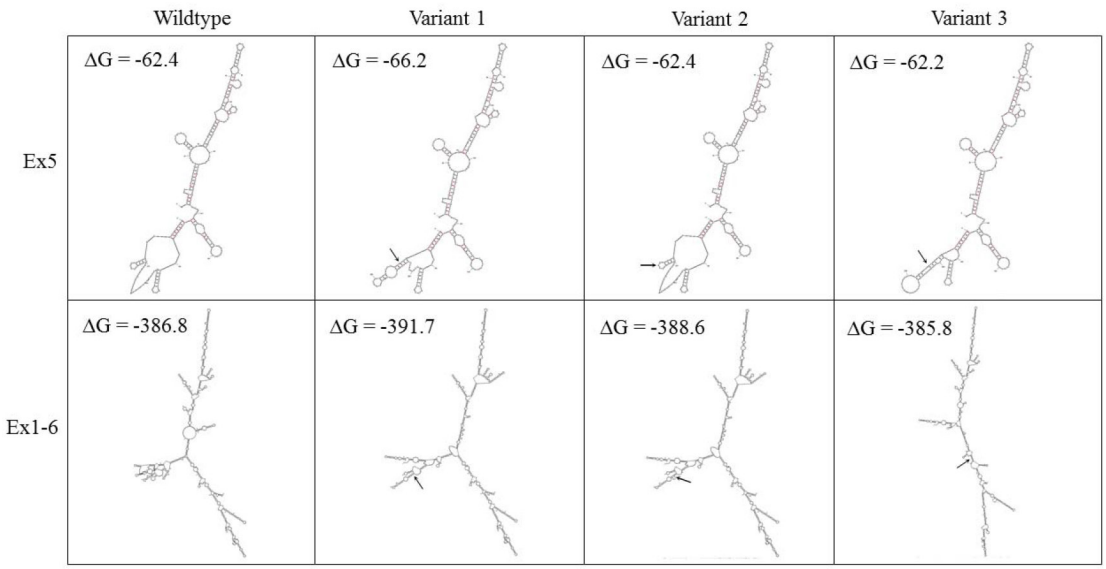

Figure 2. Predicted RNA secondary structures. The top panels show RNA folding for exon 5 only in wild-type (WT) predictions compared to those for variant 1 (V1), variant 2 (V2), and variant 3 (V3). By contrast, the bottom panels show RNA folding for full-length coding sequences for all four RNAs. The Gibbs free energy values (ΔG) for each prediction are indicated in units of kcal mol^{-1}. The arrows represent the location of the three *OPN1LW* gene variants.

Effect of variant sequences on RNA processing: The above data suggest that the RNA splicing of both intron 4 or intron 5 is unaffected by any of the single-nucleotide changes in exon 5 of the *OPN1LW* gene identified in this study. Therefore, the hypothesis that changes occur to the RNA secondary structure in the presence of variant sequences was tested in order to examine whether such changes might alter RNA stability. Initially, this was investigated using mfold [37, 38] to predict the RNA secondary structures of the region of the *OPN1LW* mRNA that encompasses exon 5 only (Figure 2, top panels).

Structurally, WT and V2 were visibly similar, as were V1 and V3. A closer inspection of the re-evaluated ΔG values [37, 38] showed that, while WT, V2, and V3 were almost identical, with free energies at −62.4 kcal mol^{-1}, −62.4 kcal mol^{-1}, and −62.2 kcal mol^{-1}, respectively, V1 was predicted to possess a ΔG value of −66.2 kcal mol^{-1} (Figure 2, top panels). This latter result suggested that more energy is required to negotiate the stem-loops contained within exon 5. As such, ribosomal coverage of the downstream region of the transcript will be less during translation at steady-state levels [39, 40], thereby leaving V1 mRNA transcripts more susceptible to nuclease attack and the removal of aberrant mRNAs by nonsense-mediated decay (NMD) [41, 42]. Although this result is consistent with the conjecture that overall mRNA instability explains the very low levels of V1 expression, as determined by qPCR, studying exon 5 in isolation did not offer a mechanism for the presence of reduced levels of V2 transcripts compared to the levels of WT and V3 transcripts.

To further investigate the effect of the three variants on RNA secondary structure and stability, predictions were made within the context of full-length post-spliced transcripts (because splicing is not affected in this study) comprising exons 1 to 6 (Figure 2, bottom panels). Although the 5′- and 3′-UTRs were not included in the transcription products, it is highly probable that they do not play a role, as they are identical across WT and all three variant RNAs. Thus, despite their absence, the analysis of full-length coding sequences represents a more biologically relevant context than does using a mini-gene approach, as previously shown [43-45]. When compared, the free energies for WT (ΔG = −386.8 kcal mol^{-1}) and V3 (ΔG = −385.8 kcal mol^{-1}) were similar (Figure 2, bottom panels), but consistent with analysis of exon 5; V1 had a greater free energy value (ΔG = −391.7 kcal mol^{-1}), suggesting that this transcript forms an RNA secondary structure with stem-loops that are more resistant to the helicase activity of the translation ribosomal complex and, as such, are more labile. In contrast to the exon 5 prediction for V2, the analysis of the full-length coding sequence showed a free energy value for V2 (ΔG = −388.6 kcal mol^{-1}) closer to that of V1 (ΔG=-391.7 kcal mol^{-1}) than to either WT (ΔG = −386.8 kcal mol^{-1}) or V3 (ΔG = −385.8 kcal mol^{-1}). Visually, the RNA secondary structure predictions showed that V1 and V2 were almost identical, with three distinct and prominent

branches, whereas WT (two main branches and a minor third branch) and V3 (two main branches) were markedly different from either V1 or V2. Overall, therefore, it appears that the RNA secondary structure predictions for full-length coding sequences for V1 and V2 differ from those of WT and V3.

DISCUSSION

This study represents the largest survey of *OPN1LW* gene variation in individuals with normal color vision. The extensive sequence variation across myopic individuals and controls in both cohorts confirmed the very high frequency of variation in the *OPN1LW* gene. Aberrant splicing in BED depends on particular nucleotides being present at five sites in exon 3, 457 in codon 153, 511 in codon 171, 521 in codon 174, 532 in codon 178, and 538 in codon 180. Variants were found at each of these sites in the present study, but none possessed the full BED haplotype or were uniquely found in myopic individuals.

Three variants, all in exon 5 in adjacent codons 324 and 325, were found uniquely in myopic individuals, all within the Raine Study. The levels of unspliced and spliced *OPN1LW* gene transcripts produced in transfected HEK293 cells, from constructs individually containing each of the three variants, did not differ from those produced from the WT construct. It is unlikely therefore that any of these variants affect the efficiency of the removal of either intron 4, intron 5 or both introns by splicing. What is evident, however, is that two of the variants, V1 and V2, resulted in a substantial reduction in the abundance of *OPN1LW* gene transcripts.

Steady-state mRNA levels (turnover) result from the rate of transcription versus the rate of mRNA decay. Given the experimental setup, the former was identical across all four groups, and any difference in cell number was corrected for by the normalization step of the qPCR pipeline. Thus, differences in overall levels of spliced transcript must be due to the rate of decay via changes in relative mRNA stability. Analyses of RNA secondary structure suggest that more stable folding requires more energy for the translational ribosomal machinery to negotiate stem-loop structures. At steady-state levels, this means that fewer ribosomes will cover the transcript (especially toward the 3′ end), thus increasing the probability of degradation (i.e., RNA folding is more stable/stronger, but stability is decreased). A study of the potential effects of these single-nucleotide substitutions on RNA secondary structure predictions for full-length coding sequences indicated that the folding of V1 and V2 is distinctly different from that of WT and V3. This may, therefore, induce significant effects on transcript stability and overall steady-state expression levels.

Evidence that this reduction in the level of opsin transcripts would lead to a comparative drop in opsin protein and, hence, in functional *OPN1LW* gene photopigment, derives from three sources. First, mutations in RNA splicing factors are known to cause dominant forms of retinitis pigmentosa [46-50], and in vitro studies have shown that the splicing of opsin transcripts is significantly affected [51]; the presence of photoreceptor loss in these disorders implies, therefore, that reduced mRNA levels translate into a decreased amount of photopigment, which is a contributing factor in the disease. Second, there is a continuing demand for opsin production to replenish the loss arising from the diurnal degradation of cone photoreceptor outer segments [52]; any reduction in the level of normal transcripts will likely translate into diminished amounts of opsin protein and functional photopigments. Last, the impact of a reduction in *OPN1LW* gene transcripts on cone photoreceptor function is evident from studies of BED, where a reduced abundance of normal transcript results in dichromacy and a significant reduction in the number of functional cones in the retina of affected individuals [53]. Indeed, the latter is correlated with the severity of myopia present in affected individuals.

A similar, but less severe, mechanism may be present, therefore, in individuals carrying either V1 or V2 variants in their *OPN1LW* gene, and this may be a causative factor in the development of myopia. Any significant reduction in the number of photopigments in cone photoreceptors may interfere with the process of emmetropization. High-acuity photopic vision provides the signals that guide emmetropization, and these are initiated by light absorption of the photopigments found in *OPN1LW* and *OPN1MW* cones. Even minor changes may have an impact on this process, leading to alterations in the process of emmetropization and the development of myopia. In the absence, however, of quantitative measurements of the number of *OPN1LW* gene photopigments present in the retina of individuals carrying either V1 or V2 cone opsin variants, it remains unclear whether this is sufficient to cause myopia. Nonetheless, the direct link between transcript exonic variants and ocular disorders could be addressed by studying animal models carrying modified *OPN1LW* genes that incorporate these variants.

APPENDIX 1. LIST OF PRIMERS USED IN THE STUDY.

To access the data, click or select the words “Appendix 1.”

APPENDIX 2. NUCLEOTIDE VARIATION IN THE *OPN1LW* CONE OPSIN GENE IN THE STUDY COHORTS.

To access the data, click or select the words "Appendix 2."

ACKNOWLEDGMENTS

Contributions of authors: Designing the study (DMH, WILD), conducting the study (JKM, WILD); collecting and managing the data (DAM, LRG, SY), preparing, reviewing the approving the manuscript (DMH, WILD, JKM, DAM, LRG, SY). ACKNOWLEDGMENTS This work was supported by an NHMRC Grant (1,030,148) awarded to DMH and DAM. Further support was provided by the Australian Research Council (ARC) in the form of a Future Fellowship (FT110100176) awarded to WILD and a Discovery Project grant (DP140102117) awarded to WILD and DMH. We are grateful to the Western Australian Pregnancy Cohort (Raine) Study participants and their families, and we thank the Raine Study and Lions Eye Institute research staff for cohort coordination and data collection. The core management of the Raine Study is funded by The University of Western Australia (UWA), Curtin University, The Telethon Kids Institute, the Raine Medical Research Foundation (UWA), the Women's and Infant's Research Foundation, Edith Cowan University, Murdoch University and The University of Notre Dame. The 20 year eye follow-up of Raine Study was funded by NHMRC Grant 1,021,105, the Ophthalmic Research Institute of Australia (ORIA), the Alcon Research Institute, the Lions Eye Institute and the Australian Foundation for the Prevention of Blindness. SY is supported by NHMRC CJ Martin Early Career Fellowship. We also thank the Norfolk Islanders for their participation in the Norfolk Island Eye Study (NIES), as well as additional NIES team members. Financial support was provided by the Royal Victorian Eye and Ear Hospital research committee, and the Peggy and Leslie Cranbourne Foundation.

REFERENCES

1. Kempen JH, Mitchell P, Lee KE, Tielsch JM, Broman AT, Taylor HR, Ikram MK, Congdon NG, O'Colmain BJ. The prevalence of refractive errors among adults in the United States, Western Europe, and Australia. Arch Ophthalmol 2004; 122:495-505. [PMID: 15078666].

2. Wensor M, McCarty CA, Taylor HR. Prevalence and risk factors of myopia in Victoria, Australia. Arch Ophthalmol 1999; 117:658-63. [PMID: 10326965].

3. Lam CS, Goldschmidt E, Edwards MH. Prevalence of myopia in local and international schools in Hong Kong. Optom Vis Sci 2004; 81:317-22. [PMID: 15181356].

4. Woo WW, Lim KA, Yang H, Lim XY, Liew F, Lee YS, Saw SM. Refractive errors in medical students in Singapore. Singapore Med J 2004; 45:470-4. [PMID: 15455167].

5. Dolgin E. The myopia boom. Nature 2015; 519:276-8. [PMID: 25788077].

6. Hornbeak DM, Young TL. Myopia genetics: a review of current research and emerging trends. Curr Opin Ophthalmol 2009; 20:356-62. [PMID: 19587595].

7. Kiefer AK, Tung JY, Do CB, Hinds DA, Mountain JL, Francke U, Eriksson N. Genome-wide analysis points to roles for extracellular matrix remodeling, the visual cycle, and neuronal development in myopia. PLoS Genet 2013; 9:e1003299-[PMID: 23468642].

8. Li J, Gao B, Guan L, Xiao X, Zhang J, Li S, Jiang H, Jia X, Yang J, Guo X, Yin Y, Wang J, Zhang Q. Unique Variants in OPN1LW Cause Both Syndromic and Nonsyndromic X–Linked High Myopia Mapped to MYP1. Invest Ophthalmol Vis Sci 2015; 56:4150-5. [PMID: 26114493].

9. Verhoeven V.J., Hysi P.G., Wojciechowski R., Fan Q., Guggenheim J.A., Hohn R., MacGregor S., Hewitt A.W., Nag A., Cheng C.Y., Yonova-Doing E., Zhou X., Ikram M.K., Buitendijk G.H., McMahon G., Kemp J.P., Pourcain B.S., Simpson C.L., Makela K.M., Lehtimaki T., Kahonen M., Paterson A.D., Hosseini S.M., Wong H.S., Xu L., Jonas J.B., Parssinen O., Wedenoja J., Yip S.P., Ho D.W., Pang C.P., Chen L.J., Burdon K.P., Craig J.E., Klein B.E., Klein R., Haller T., Metspalu A., Khor C.C., Tai E.S., Aung T., Vithana E., Tay W.T., Barathi V.A.. Consortium for Refractive, E., Myopia, Chen, P., Li, R., Liao, J., Zheng, Y., Ong, R.T., Doring, A., Diabetes, C., Complications Trial/Epidemiology of Diabetes, I., Complications Research, G., Evans, D.M., Timpson, N.J., Verkerk, A.J., Meitinger, T., Raitakari, O., Hawthorne, F., Spector, T.D., Karssen, L.C., Pirastu, M., Murgia, F., Ang, W., Wellcome Trust Case Control, C., Mishra, A., Montgomery, G.W., Pennell, C.E., Cumberland, P.M., Cotlarciuc, I., Mitchell, P., Wang, J.J., Schache, M., Janmahasatian, S., Igo, R.P., Jr., Lass, J.H., Chew, E., Iyengar, S.K., Fuchs' Genetics Multi-Center Study, G., Gorgels, T.G., Rudan, I., Hayward, C., Wright, A.F., Polasek, O., Vatavuk, Z., Wilson, J.F., Fleck, B., Zeller, T., Mirshahi, A., Muller, C., Uitterlinden, A.G., Rivadeneira, F., Vingerling, J.R., Hofman, A., Oostra, B.A., Amin, N., Bergen, A.A., Teo, Y.Y., Rahi, J.S., Vitart, V., Williams, C., Baird, P.N., Wong, T.Y., Oexle, K., Pfeiffer, N., Mackey, D.A., Young, T.L., van Duijn, C.M., Saw, S.M., Bailey-Wilson, J.E., Stambolian, D., Klaver, C.C., Hammond, C.JGenome-wide meta-analyses of multiancestry cohorts identify multiple new susceptibility loci for refractive error and myopia. Nat Genet 2013; 45:314-8. [PMID: 23396134].

10. Young TL, Deeb SS, Ronan SM, Dewan AT, Alvear AB, Scavello GS, Paluru PC, Brott MS, Hayashi T, Holleschau AM, Benegas N, Schwartz M, Atwood LD, Oetting WS, Rosenberg T, Motulsky AG, King RA. X-linked high myopia associated with cone dysfunction. Arch Ophthalmol 2004; 122:897-908. [PMID: 15197065].

11. Schwartz M, Haim M, Skarsholm D. X-linked myopia: Bornholm eye disease. Linkage to DNA markers on the distal part of Xq. Clin Genet 1990; 38:281-6. [PMID: 1980096].

12. Michaelides M, Johnson S, Bradshaw K, Holder GE, Simunovic MP, Mollon JD, Moore AT, Hunt DM. X-linked cone dysfunction syndrome with myopia and protanopia. Ophthalmology 2005; 112:1448-54. [PMID: 15953640].

13. McClements M, Davies WI, Michaelides M, Young T, Neitz M, MacLaren RE, Moore AT, Hunt DM. Variations in opsin coding sequences cause x–linked cone dysfunction syndrome with myopia and dichromacy. Invest Ophthalmol Vis Sci 2013; 54:1361-9. [PMID: 23322568].

14. Ueyama H, Muraki-Oda S, Yamade S, Tanabe S, Yamashita T, Shichida Y, Ogita H. Unique haplotype in exon 3 of cone opsin mRNA affects splicing of its precursor, leading to congenital color vision defect. Biochem Biophys Res Commun 2012; 424:152-7. [PMID: 22732407].

15. Gardner JC, Liew G, Quan YH, Ermetal B, Ueyama H, Davidson AE, Schwarz N, Kanuga N, Chana R, Maher ER, Webster AR, Holder GE, Robson AG, Cheetham ME, Liebelt J, Ruddle JB, Moore AT, Michaelides M, Hardcastle AJ. Three different cone opsin gene array mutational mechanisms with genotype-phenotype correlation and functional investigation of cone opsin variants. Hum Mutat 2014; 35:1354-62. [PMID: 25168334].

16. Greenwald SH, Kuchenbecker JA, Rowlan JS, Neitz J, Neitz M. Role of a Dual Splicing and Amino Acid Code in Myopia, Cone Dysfunction and Cone Dystrophy Associated with L/M Opsin Interchange Mutations. Transl Vis Sci Technol 2017; 6:2-[PMID: 28516000].

17. Orosz O, Rajta I, Vajas A, Takacs L, Csutak A, Fodor M, Kolozsvari B, Resch M, Senyi K, Lesch B, Szabo V, Berta A, Balogh I, Losonczy G. Myopia and Late-Onset Progressive Cone Dystrophy Associate to LVAVA/MVAVA Exon 3 Interchange Haplotypes of Opsin Genes on Chromosome X. Invest Ophthalmol Vis Sci 2017; 58:1834-42. [PMID: 28358949].

18. Carroll J, Neitz M, Hofer H, Neitz J, Williams DR. Functional photoreceptor loss revealed with adaptive optics: an alternate cause of color blindness. Proc Natl Acad Sci USA 2004; 101:8461-6. [PMID: 15148406].

19. Wagner-Schuman M, Neitz J, Rha J, Williams DR, Neitz M, Carroll J. Color-deficient cone mosaics associated with Xq28 opsin mutations: a stop codon versus gene deletions. Vision Res 2010; 50:2396-402. [PMID: 20854834].

20. Flitcroft DI. Emmetropisation and the aetiology of refractive errors. Eye (Lond) 2014; 28:169-79. [PMID: 24406411].

21. Li J, Gao B, Guan L, Xiao X, Zhang J, Li S, Jiang H, Jia X, Yang J, Guo X, Yin Y, Wang J, Zhang Q. Unique Variants in OPN1LW Cause Both Syndromic and Nonsyndromic X–Linked High Myopia Mapped to MYP1. Invest Ophthalmol Vis Sci 2015; 56:4150-5. [PMID: 26114493].

22. Dulai KS, von Dornum M, Mollon JD, Hunt DM. The evolution of trichromatic color vision by opsin gene duplication in New World and Old World primates. Genome Res 1999; 9:629-38. [PMID: 10413401].

23. Hunt DM, Carvahlo LS. 2016. The Genetics of Color Vision and Congenital Color Deficiencies, in: Kremers, J., Baraas, R.C., Marshall, N.J. (Eds.), Human Color Vision. Springer International Publishing, Zurich, Switzerland, pp. 1–32.

24. Straker L, Mountain J, Jacques A, White S, Smith A, Landau L, Stanley F, Newnham J, Pennell C, Eastwood P. Cohort Profile: The Western Australian Pregnancy Cohort (Raine) Study-Generation 2. Int J Epidemiol 2017; 46:1384-5. [PMID: 28064197].

25. Yazar S, Forward H, McKnight CM, Tan A, Soloshenko A, Oates SK, Ang W, Sherwin JC, Wood D, Mountain JA, Pennell CE, Hewitt AW, Mackey DA. Raine eye health study: design, methodology and baseline prevalence of ophthalmic disease in a birth-cohort study of young adults. Ophthalmic Genet 2013; 34:199-208. [PMID: 23301674].

26. Alexander C. 2003. The Bounty: The True Story of the Mutiny on the Bounty. Penguin Books Ltd, London.

27. Sherwin JC, Kelly J, Hewitt AW, Kearns LS, Griffiths LR, Mackey DA. Prevalence and Associations of Refractive Error on Norfolk Island: Norfolk Island Eye Study. Clin Experiment Ophthalmol 2011; 39:734-42. [PMID: 21631679].

28. Davies WL, Carvalho LS, Hunt DM. SPLICE: a technique for generating in vitro spliced coding sequences from genomic DNA. Biotechniques 2007; 43:785-9. [PMID: 18251255].

29. Franke RR, Sakmar TP, Oprian DD, Khorana HG. A single amino acid substitution in rhodopsin (lysine 248—-leucine) prevents activation of transducin. J Biol Chem 1988; 263:2119-22. [PMID: 3123487].

30. Davies WI, Tamai TK, Zheng L, Fu JK, Rihel J, Foster RG, Whitmore D, Hankins MW. An extended family of novel vertebrate photopigments is widely expressed and displays a diversity of function. Genome Res 2015; 25:1666-79. [PMID: 26450929].

31. Davies WI, Zheng L, Hughes S, Tamai TK, Turton M, Halford S, Foster RG, Whitmore D, Hankins MW. Functional diversity of melanopsins and their global expression in the teleost retina. Cell Mol Life Sci 2011; 68:4115-32. [PMID: 21833582].

32. Davies WL, Carvalho LS, Tay BH, Brenner S, Hunt DM, Venkatesh B. Into the blue: gene duplication and loss underlie color vision adaptations in a deep-sea chimaera, the elephant shark *Callorhinchus milii*. Genome Res 2009; 19:415-26. [PMID: 19196633].

33. Davies WL, Cowing JA, Bowmaker JK, Carvalho LS, Gower DJ, Hunt DM. Shedding light on serpent sight: the visual pigments of henophidian snakes. J Neurosci 2009; 29:7519-25. [PMID: 19515920].

34. Davies WL, Cowing JA, Carvalho LS, Potter IC, Trezise AE, Hunt DM, Collin SP. Functional characterization, tuning, and regulation of visual pigment gene expression in an anadromous lamprey. FASEB J 2007; 21:2713-24. [PMID: 17463225].

35. Vandesompele J, De Preter K, Pattyn F, Poppe B, Van Roy N, De Paepe A, Speleman F. Accurate normalization of real-time quantitative RT-PCR data by geometric averaging of multiple internal control genes. Genome Biol 2002; 3:1-11. .

36. Carleton KL, Kocher TD. Cone opsin genes of african cichlid fishes: tuning spectral sensitivity by differential gene expression. Mol Biol Evol 2001; 18:1540-50. [PMID: 11470845].

37. Mathews DH, Sabina J, Zuker M, Turner DH. Expanded sequence dependence of thermodynamic parameters improves prediction of RNA secondary structure. J Mol Biol 1999; 288:911-40. [PMID: 10329189].

38. Zuker M. Mfold web server for nucleic acid folding and hybridization prediction. Nucleic Acids Res 2003; 31:3406-15. [PMID: 12824337].

39. Davies WL, Vandenberg JI, Sayeed RA, Trezise AE. Cardiac expression of the cystic fibrosis transmembrane conductance regulator involves novel exon 1 usage to produce a unique N-terminal protein. J Biol Chem 2004; 279:15877-87. [PMID: 14754881].

40. Davies WL, Vandenberg JI, Sayeed RA, Trezise AE. Post-transcriptional regulation of the cystic fibrosis gene in cardiac development and hypertrophy. Biochem Biophys Res Commun 2004; 319:410-8. [PMID: 15178422].

41. Maquat LE. When cells stop making sense: effects of nonsense codons on RNA metabolism in vertebrate cells. RNA 1995; 1:453-65. [PMID: 7489507].

42. Wagner E, Lykke-Andersen J. mRNA surveillance: the perfect persist. J Cell Sci 2002; 115:3033-8. [PMID: 12118059].

43. Gamundi MJ, Hernan I, Muntanyola M, Maseras M, Lopez-Romero P, Alvarez R, Dopazo A, Borrego S, Carballo M. Transcriptional expression of cis-acting and trans-acting splicing mutations cause autosomal dominant retinitis pigmentosa. Hum Mutat 2008; 29:869-78. [PMID: 18412284].

44. Hernan I, Gamundi MJ, Planas E, Borras E, Maseras M, Carballo M. Cellular expression and siRNA-mediated interference of rhodopsin cis-acting splicing mutants associated with autosomal dominant retinitis pigmentosa. Invest Ophthalmol Vis Sci 2011; 52:3723-9. [PMID: 21357407].

45. van der Klift HM, Jansen AM, van der Steenstraten N, Bik EC, Tops CM, Devilee P, Wijnen JT. Splicing analysis for exonic and intronic mismatch repair gene variants associated with Lynch syndrome confirms high concordance between minigene assays and patient RNA analyses. Mol Genet Genomic Med 2015; 3:327-45. [PMID: 26247049].

46. Chakarova CF, Hims MM, Bolz H, Abu-Safieh L, Patel RJ, Papaioannou MG, Inglehearn CF, Keen TJ, Willis C, Moore AT, Rosenberg T, Webster AR, Bird AC, Gal A, Hunt D, Vithana EN, Bhattacharya SS. Mutations in HPRP3, a third member of pre-mRNA splicing factor genes, implicated in autosomal dominant retinitis pigmentosa. Hum Mol Genet 2002; 11:87-92. [PMID: 11773002].

47. Deery EC, Vithana EN, Newbold RJ, Gallon VA, Bhattacharya SS, Warren MJ, Hunt DM, Wilkie SE. Disease mechanism for retinitis pigmentosa (RP11) caused by mutations in the splicing factor gene PRPF31. Hum Mol Genet 2002; 11:3209-19. [PMID: 12444105].

48. Vithana EN, Abu-Safieh L, Allen MJ, Carey A, Papaioannou M, Chakarova C, Al-Maghtheh M, Ebenezer ND, Willis C, Moore AT, Bird AC, Hunt DM, Bhattacharya SS. A human homolog of yeast pre-mRNA splicing gene, PRP31, underlies autosomal dominant retinitis pigmentosa on chromosome 19q13.4 (RP11). Mol Cell 2001; 8:375-81. [PMID: 11545739].

49. Wilkie SE, Morris KJ, Bhattacharya SS, Warren MJ, Hunt DM. A study of the nuclear trafficking of the splicing factor protein PRPF31 linked to autosomal dominant retinitis pigmentosa (ADRP). Biochim Biophys Acta 2006; 1762:304-11. [PMID: 16427773].

50. Wilkie SE, Vaclavik V, Wu H, Bujakowska K, Chakarova CF, Bhattacharya SS, Warren MJ, Hunt DM. Disease mechanism for retinitis pigmentosa (RP11) caused by missense mutations in the splicing factor gene PRPF31. Mol Vis 2008; 14:683-90. [PMID: 18431455].

51. Yuan L, Kawada M, Havlioglu N, Tang H, Wu JY. Mutations in PRPF31 inhibit pre-mRNA splicing of rhodopsin gene and cause apoptosis of retinal cells. J Neurosci 2005; 25:748-57. [PMID: 15659613].

52. Kocaoglu OP, Liu Z, Zhang F, Kurokawa K, Jonnal RS, Miller DT. Photoreceptor disc shedding in the living human eye. Biomed Opt Express 2016; 7:4554-68. [PMID: 27895995].

53. Patterson EJ, Wilk M, Langlo CS, Kasilian M, Ring M, Hufnagel RB, Dubis AM, Tee JJ, Kalitzeos A, Gardner JC, Ahmed ZM, Sisk RA, Larsen M, Sjoberg S, Connor TB, Dubra A, Neitz J, Hardcastle AJ, Neitz M, Michaelides M, Carroll J. Cone Photoreceptor Structure in Patients With X–Linked Cone Dysfunction and Red-Green Color Vision Deficiency. Invest Ophthalmol Vis Sci 2016; 57:3853-63. [PMID: 27447086].

Articles are provided courtesy of Emory University and the Zhongshan Ophthalmic Center, Sun Yat-sen University, P.R. China. The print version of this article was created on 17 March 2019. This reflects all typographical corrections and errata to the article through that date. Details of any changes may be found in the online version of the article.